applied sciences

MDPI

Article

A Screw-Axis Approach to the Stability of Two-Wheeled Vehicles

Matteo Bova and Matteo Massaro *

Department of Industrial Engineering, University of Padova, Via Venezia 1, 35131 Padova, Italy; matteo.bova@phd.unipd.it

* Correspondence: matteo.massaro@unipd.it

Abstract: The stability of two-wheeled vehicles is predominantly characterized by the well-known weave and wobble vibration modes, which have been extensively investigated in the literature, mainly in terms of their frequencies and damping ratios. In this work the focus is towards their mode shapes, which are investigated using the screw-axis (also called Mozzi-axis), instead of the classic compass diagrams, for a better understanding of their three-dimensional patterns. The analysis is then carried out using the velocity centres for a characterization from the top, rear and side view of the vehicle. The multibody vehicle model employed for the numerical analysis is built in Adams. The dataset resembles that of a 250cc sport motorcycle, and has been derived from laboratory tests. The stability analysis is carried out in the frequency domain. It is found that, depending on the selected plane for the projection of the three-dimensional vibration motion, the trajectories of the velocity centres of the weave and wobble can cross either aft or fore the centre of mass, which has been associated to the under- and over-steering behaviour in the literature.

Keywords: motorcycle; rider; screw axis; weave; wobble; multibody

Citation: Bova, M.; Massaro, M. A Screw-Axis Approach to the Stability of Two-Wheeled Vehicles. *Appl. Sci.* **2021**, *11*, 7393. https://doi.org/10.3390/app11167393

Academic Editors: Flavio Farroni, Andrea Genovese and Aleksandr Sakhnevych

Received: 30 June 2021
Accepted: 10 August 2021
Published: 11 August 2021

1. Introduction

The lateral stability of two-wheeled vehicles has been investigated extensively in the last 50 years, both numerically and experimentally. It is well known that there are two main vibration modes, namely weave and wobble [1–6]. Weave is characterized by steering oscillations combined with yaw, roll and lateral motion of the vehicle, with frequencies usually below 4–5 Hz, while wobble is dominated by steering oscillation, with frequency usually in the range 6–10 Hz. Weave is usually lightly damped at high speed, say above 100 km/h, while wobble tends to be lightly damped at low to medium speed, although such range is affected by the structural stiffness of the vehicle [7,8].

The effect of a rider on the vehicle stability has also been investigated. Historically, the rider has been assumed to be rigidly attached to the chassis, with the inertial properties estimated using prediction-regression formulas from biomechanical databases. A number of different sources are available in the literature, with a review of the most used given in [9].

Starting from the mid 1980s, the rider's passive motion on the saddle has been modelled using spring-damper elements tuned to give the typical modal properties obtained from experiments [10–13]. More recently, the effect related to 'hands-on' and 'hands-off' the handlebar has been investigated. Experiments aimed at the identification of the rider–steering interaction has been carried out [14,15]. The numerical simulations and the experiments suggest that with hands on the handlebar wobble becomes more stable, while weave destabilizes [16–18].

Most of the analyses mentioned above focus on the effect that the main vehicle, tyre and rider parameters have on the frequency and damping of the vibration modes. Such modes are usually presented in terms of the real and imaginary part of the eigenvalues—which are related to the damping and frequency of the vibration modes—as a function of the vehicle speed. In contrast, the focus of this work is on the shape of the vibration modes.

The underlying idea is that, given the same combination of frequency and damping ratio, the vehicle may be perceived to be more or less stable by the rider depending on the shape of the vibration modes. In order to characterize the mode shape, the screw-axes associated to the weave and wobble are computed, in addition to the compass diagrams, which are the standard to describe the mode shape. It is recalled that each motion in the space, e.g., that of the chassis of a two-wheeled vehicle, can be represented (instantaneously) as a rotation around and a translation along a screw-axis, also called Mozzi axis [19,20]. The direction of the screw axis coincides with the (instantaneous) direction of the angular velocity vector. The intersection between the screw axis and a reference plane gives the velocity centres of the motion projected on that reference plane. Two planes are considered in this work: transverse plane (motion observed from the top of the vehicle) and frontal plane (motion observed from the front of the vehicle). The side view is not interesting in the case of straight-motion analysis. Indeed, it is well know that in such a condition weave and wobble modes do not involve either suspension oscillations or tyre radial oscillations, as long as the vehicle is symmetric (which is the case on most models, including the one considered in this work).

The screw axis has been previously employed to analyse the motion of motorcycles during slalom [21], lane-change and turning [22], and lap simulation [23]. More recently, velocity centres have been used to investigate the mode shape of the weave mode [24]. In this work, such analysis is generalized through the screw-axis and extended to include also the front view and wobble.

The work is organized as follows. Section 2 describes the vehicle model employed and discusses its vibration modes, in order to show its consistency with other results reported in the literature. Section 3 recalls the formulas related to the computation of the screw axis and velocity centres. Section 4 is devoted to the analysis of the shape of the weave mode, while in Section 5 the wobble mode is considered.

2. Multibody Model

The multibody model is built in Adams, which is one of the most used environments for vehicle dynamic analysis. The motorcycle model is standard, including the eleven degrees of freedom associated to the gross motion (chassis position and orientation, steering rotation, suspension travels and wheels rotation). The modelling of the structural compliance is limited to the lateral bending and torsion of the chassis (one additional degree of freedom), which is well known to be essential for a proper modelling of the vibration modes [5,7,8]. The tyres are modelled using the Magic Formula approach [5], which is included in Adams by default. The inertial properties of the bike were measured in the laboratory of the University of Padova, while the rider inertial properties were estimated using the Zatsiorsky–DeLeva dataset, which is one the most used [9]. The hands are assumed to be off the handlebar [16].

The vibration properties are usually extracted in two alternative ways: Using a time domain simulation or a frequency domain simulation. The former case resembles the approach employed also during experimental tests, where the system is excited using an impulse (e.g., on the handlebar) and the resulting oscillation is analysed in order to extract its modal component. The latter approach—frequency domain—is the preferred approach in this work, because it allows to compute the vibration properties more efficiently. In practice, all of the vibration modes are extracted simultaneously without applying any impulse on the system. The following procedure is carried out at all the speeds of interest.

A time domain simulation is started at the speed of interest using a proportional-derivative-integral (PID) engine torque controller to keep the vehicle at constant speed (the observed variable is the speed error): Indeed, at least the aerodynamic drag and the rolling resistance need to be balanced. The simulation is stopped when a steady-state condition is reached, i.e., when the transient oscillations have disappeared (which usually happen after

3–5 s). At this stage the PID is disengaged and the plant linearised in order to obtain the standard state space formulation

$$\dot{x} = Ax + Bu \quad (1)$$
$$y = Cx + Du \quad (2)$$

where A is the state matrix, B is the input matrix, C is the output matrix and D is the feed-through matrix; y denotes the observed variables, u are the inputs (steering torque and engine torque) and x are the model states:

$$x = [\dot{X}, X, \dot{Y}, Y, \dot{Z}, Z, \dot{\phi}, \phi, \dot{\theta}, \theta, \dot{\psi}, \psi, \dot{\delta}, \delta, \dot{\xi}_r, \xi_r, \dot{\xi}_f, \xi_f, \dot{\beta}_r, \beta_r, \dot{\beta}_f, \beta_f, \dot{\gamma}, \gamma, \sigma_1, \cdots, \sigma_9]^T. \quad (3)$$

The model has 31 states: The first 24 states in (3) consists of the 12 user selected position states (which are manually defined through the PSTATE command in Adams) and their derivatives, while the latter seven states are automatically generated by Adams and are likely associated to the (transient) Magic Formula tyre model (e.g., longitudinal and lateral relaxation equations of the front and rear tyres) and other internal variables not directly controlled by the user. In more detail, in the user-selected states X, Y and Z are the longitudinal, lateral and vertical displacements of the saddle position (however any other point of the chassis works equally fine), ϕ, θ and ψ are the roll, pitch and yaw angles of the saddle reference marker (i.e., of the chassis, since it is assumed rigid), δ is the steering angle, ξ_r and ξ_f are the rear and front suspension deformations, β_r and β_f are the rear and front wheel spin angles and γ is the bending deflection of the front frame [7,8], while $\sigma_1, \cdots, \sigma_9$ are the states automatically generated by Adams. It is noted that the controller is disengaged before linearising the system, in order to obtain the open-loop dynamics, i.e., the dynamics of the bike and not those of the bike-controller combination (in addition, one would have more states in (3) in the case the PID is still engaged at the time of the linearization). The procedure is automated using an Adams *macro*, which is then called from a Matlab script. The vibration modes consist of the (complex) eigenvalues of the state matrix A, with the mode shape being the related (complex) eigenvectors.

Figure 1 shows the root-locus (imaginary vs. real part of the eigenvalues) of the vehicle under investigation, for speeds between 5 (circles) and 50 m/s (squares). It goes without saying that there are as many eigenvalues as the number of states in (3)—as usual only the upper half of the root-locus diagram is shown because it is symmetric with respect to the x-axis. Two 'high' frequency modes can be seen above 13.5 Hz (85 rad/s), corresponding to the front and rear wheel hop, respectively—the former mainly involves the bouncing of the front wheel on the road, while the latter mainly involves the bouncing of the rear wheel on the road. They are marginally affected by the speed variations, the rear hop mode being mainly affected in terms of frequency (which slightly decreases at high speed), the front hop mode being mainly affected in terms of damping (which slightly decreases with speed). The rear wobble mode is visible below the hop modes, with a damping increasing with the speeds, while its frequencies decrease with speed from 9.5 Hz (60 rad/s) to 0 Hz (non-vibrating). This mode is usually not very interesting because it is always stable. Wobble is a mode mainly involving steering oscillations, with frequencies decreasing from 8.5 Hz (53 rad/s) to 5.5 Hz (35 rad/s) in this vehicle. Weave is a mode involving the lateral degrees-of-freedom of the vehicle, and has frequencies rising with speeds from 0.5 Hz (3 rad/s) up to 5 Hz (31 rad/s). On the horizontal axis there is the capsize mode: It does not vibrate, is lightly unstable at low speeds (in this vehicle), and mainly involves the roll and lateral degrees of freedom. Finally, the modes associated with the suspension dynamics are visible at lower frequencies: Bounce (or heave) has frequencies around 2.4 Hz (15 rad/s), while pitch has frequencies around 3.2 Hz (20 rad/s). As a recap, the modes of the vehicle in straight running can be divided into two categories: In-plane modes (namely bounce, pitch and hops) and out-of-plane modes (namely capsize, rear wobble, wobble and weave). The latter modes are the most interesting for the current analysis, because they have implications on the running stability of two-wheeled vehicles. Weave is also one

of the most investigated modes, because it is lightly damped in many vehicles when the speed is high enough.

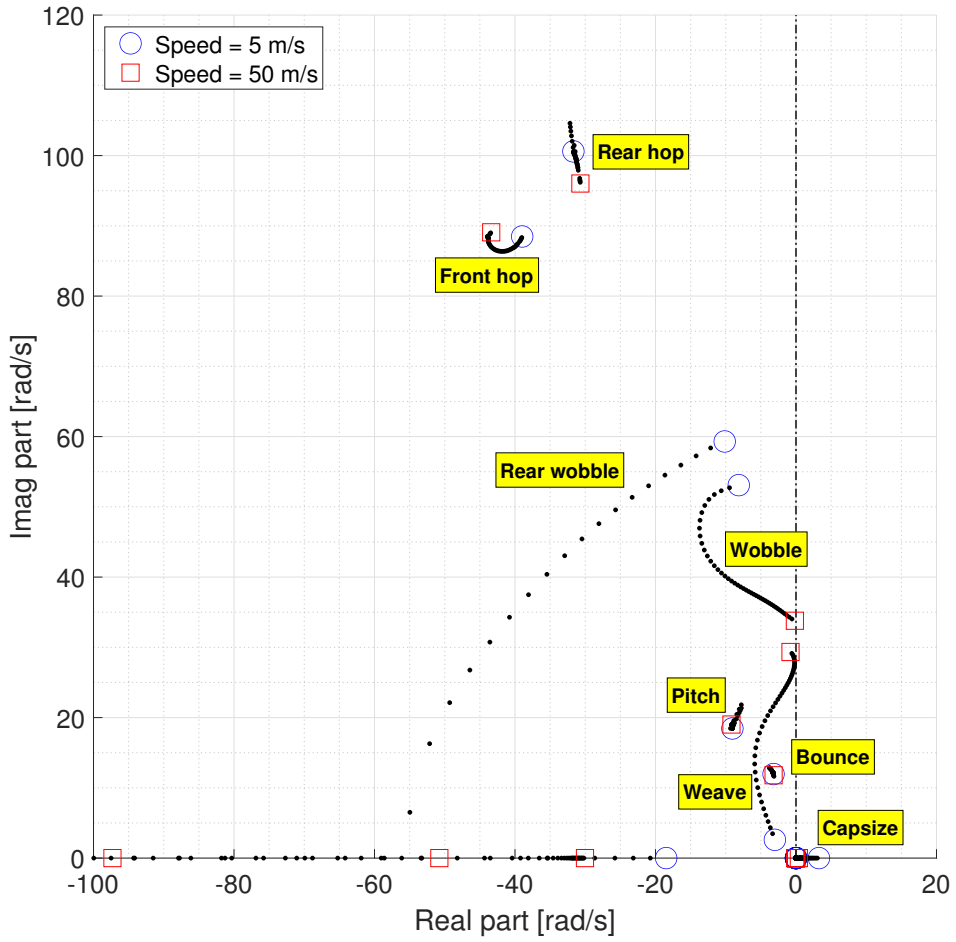

Figure 1. Vibration modes for speeds between 5 m/s (circle) and 50 m/s (square).

Figure 2 shows the compass plots of the weave mode shape: The length of each arrow represents the magnitude of the associated degree of freedom, with the related phase being the angle with respect to the horizontal axis. It is recalled that, as is common in vibration analysis, only the ratio between the magnitudes and the relative angles matter. The shape of the weave mode at high speed is similar to other results reported in the literature, with yaw almost in phase opposition with respect to the steering, roll in between the steer and yaw, while the steer lags with respect to the lateral motion [8,12,24]—an SAE conventions is employed, i.e., the z axis (both yaw and steer) points downward and the x axis points forward, while the y (lateral) axis completes the orthogonal triad. At low speeds all the four main degrees of freedom involved have similar magnitudes, with the roll (ϕ) prevailing on the others, while at high speeds the steer angle (δ) becomes dominant (however, there are still visible components of the other degrees-of-freedom).

It is recalled that in [24] two main types of weave shapes are defined: When the yaw (ψ) is in phase with the lateral displacement (y) the weave is called "under-steering" (the centrode intersection falls behind the centre of mass, as will be discussed in Section 3), otherwise the weave is called "over-steering" (the centrode intersection falls ahead of the centre of mass) and represents the case discussed in this work and shown in Figure 2. It is also said that "under-steering" scenarios are associated with an increased perception of safety.

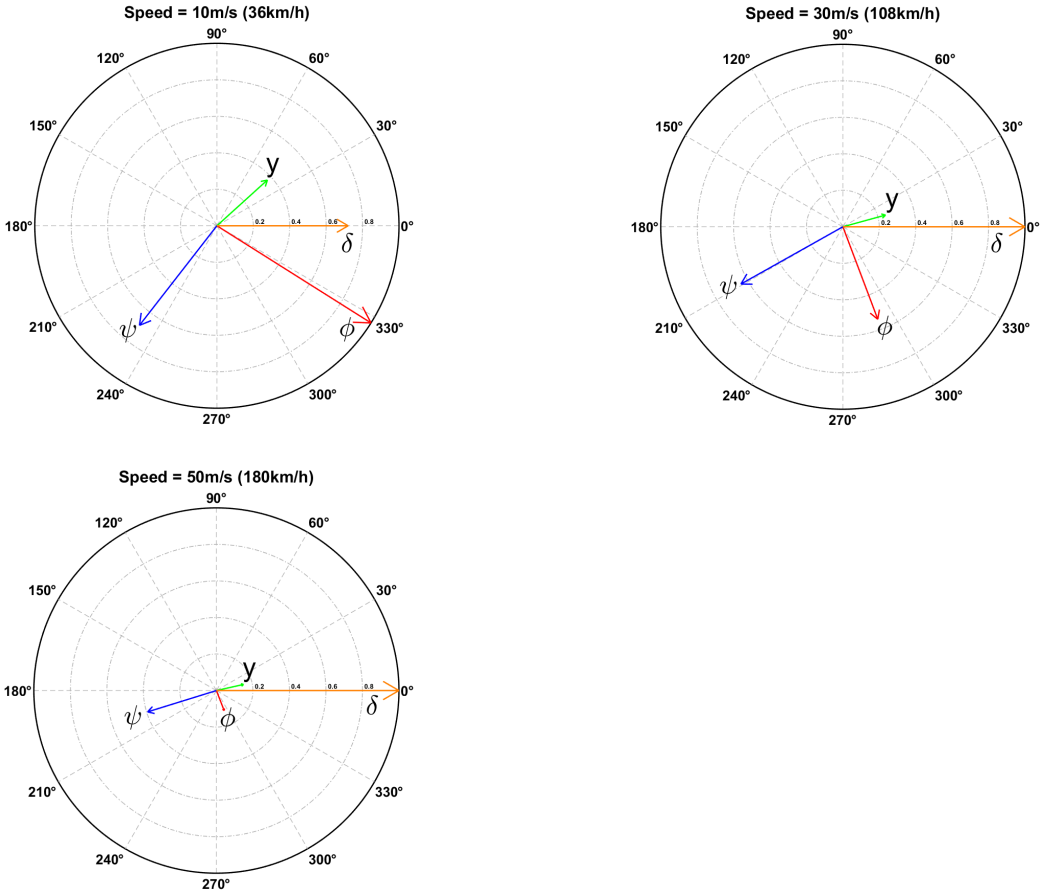

Figure 2. Weave compass diagrams at different speeds: y is the saddle point lateral displacement, δ is the steer angle, ϕ is the roll angle and ψ is the yaw angle.

3. Screw-Axis and Velocity Centres

The screw axis of the chassis is computed from the eigenvectors of the state matrix A in (1), which can be 'animated' in the time domain through

$$x(t) = x_0 e^{-\omega_n \zeta t} \sin\left[\left(\sqrt{1-\zeta^2}\right)\omega_n t + \phi\right], \tag{4}$$

where x_0 is the magnitude of the eigenvector state (i.e., the length of the arrow of the compass plot), ω_n is the (undamped) frequency of the corresponding eigenvalue, ζ is the damping ratio of the corresponding eigenvalue, ϕ is the phase (i.e., the angle of the arrow of the compass plot), and t is the time. Each point P_0 of the chassis has a velocity v_0 and angular velocity ω during the oscillation—the latter is the same for each point of the chassis, which is here treated as a rigid body. The velocity v_0 can be divided in two different components: $v_\parallel$ parallel to ω and $v_\perp$ normal to ω, which are given by

$$v_\parallel = \left(v_0 \cdot \frac{\omega}{\|\omega\|}\right)\frac{\omega}{\|\omega\|} \tag{5}$$

$$v_\perp = v_0 - v_\parallel \tag{6}$$

The normal component can also be written as

$$v_\perp = \omega \times d, \tag{7}$$

where d is the distance between the screw axis and P_0. When multiplying both sides by ω one obtains

$$v_\perp \times \omega = (\omega \times d) \times \omega, \tag{8}$$

which can be rewritten using triple-product identity as

$$\begin{aligned} v_\perp \times \omega &= (\omega \cdot \omega)d - (d \cdot \omega)\omega & (9)\\ &= \|\omega\|^2 d. & (10) \end{aligned}$$

Therefore, the distance d can be computed at each instant from

$$d = \frac{v_\perp \times \omega}{\|\omega\|^2}, \tag{11}$$

while the equation of the screw axis is given by

$$\begin{aligned} S_a &= P_0 - d + \mu\omega, & (12)\\ \begin{pmatrix} x_a \\ y_a \\ z_a \end{pmatrix} &= \begin{pmatrix} x_0 \\ y_0 \\ z_0 \end{pmatrix} - \frac{1}{\omega_x^2 + \omega_y^2 + \omega_z^2} \begin{pmatrix} -v_z\omega_y + v_y\omega_z \\ -v_x\omega_z + v_z\omega_x \\ -v_y\omega_x + v_x\omega_y \end{pmatrix} + \mu \begin{pmatrix} \omega_x \\ \omega_y \\ \omega_z \end{pmatrix} & (13) \end{aligned}$$

where μ is a scalar associated with the infinite points of the screw axis line.

The three-dimensional motion of the chassis can be projected on an $x-y$ transverse plane (parallel to the road plane, i.e., top view), a $y-z$ frontal plane (i.e., front view) or an $x-z$ sagittal plane (i.e., side view). In this case the screw axis is replaced by the velocity centre, whose trajectory on the selected plane can be obtained by intersection between the screw line and the selected plane. The scalar μ corresponding to the transverse plane is obtained when solving the third equation in (13) for $z_a = z_S$, with z_S being the height of the selected plane:

$$\mu = \frac{1}{\omega_z}\left(z_S - z_0 - \frac{v_y\omega_x - v_x\omega_y}{\omega_x^2 + \omega_y^2 + \omega_z^2}\right). \tag{14}$$

Similarly, the scalar μ corresponding to the projection on the frontal plane is given by

$$\mu = \frac{1}{\omega_x}\left(x_M - x_0 - \frac{v_z\omega_y - v_y\omega_z}{\omega_x^2 + \omega_y^2 + \omega_z^2}\right), \tag{15}$$

which is obtained from the second of (13) in the case $x_a = x_S$, with x_S being the coordinate of the selected plane. Finally, the intersection with the sagittal plane is not considered, since in straight motion the lateral modes are decoupled from the longitudinal modes: As a consequence $\omega_y = 0$ (pitch rate) during weave and wobble, and the screw axis remains parallel to the vehicle sagittal plane.

In principle, the approach presented can also be applied to experimental data, i.e., logged from the IMU of the vehicle, in addition to numerical data. The approach has shown to be able to work in two-dimensional scenarios (velocity centres), as demonstrated in [24]. From the practical point of view, the mode shape need be extracted first. When the problem is attacked numerically, it is convenient to extract the mode shape from the linearisation of the system (frequency domain approach). When the problem is attacked experimentally, a time domain approach is usually the preferred choice, i.e., the time signals are fitted to build the mode shape. Once the mode shape is obtained, the method makes no distinction on their numerical or experimental origin. In general, the approach presented is expected to work well if the mode shape is computed well.

4. Weave Analysis

In this section the weave mode shape is analysed in three transverse (top view) and three frontal (front view) planes, at different speeds. For the graphical representation of the velocity centre trajectories, the eigenvector has been normalized to have a saddle point lateral displacement equal to 0.5 m. However, the scaling does not affect the position of the cross points either on the transverse or frontal planes.

4.1. Top-View

Figure 3 shows the trajectory of the velocity centre (centrode) during the weave oscillation, when the transverse plane considered is through the saddle (which in this case is at 0.8 m from the road on static condition). The pattern changes with the speed: At 10 m/s the trajectories cross between the handlebar and the centre of mass at 0.795 m from the rear contact point, while at 30 m/s and 50 m/s the cross point shifts towards the rear contact point at 0.633 m and 0.623 m, respectively. Following the nomenclature introduced in [24], such a condition is called over-steering weave (centrode intersection ahead of the centre of mass, which is at 0.6 m from the rear contact point on static condition).

However, the centrode intersection changes when considering different transverse planes. Another option is to choose a plane through the centre of mass (which in this case is at 0.58 m from the road on static condition), see Figure 4. In this case the intersections exhibit the same behaviour mentioned above, moving from 0.709 m at 10 m/s to 0.615–0.613 m at 30 and 50 m/s, respectively, getting closer to the centre of mass while remaining still ahead of it (over-steering weave).

Yet another option is to consider the projection on the road plane. In this case the results are those in Figure 5: The intersection appears behind the centre of mass, moving closer to it from 0.479 m to 0.568–0.587 m at 10, 30 and 50 m/s, respectively—following the nomenclature introduced in [24] this weave is called under-steering.

The saddle plane may be a good choice if one is willing to associate the shape of the mode to the rider's feeling and perceived stability. On the other hand, the centre of mass plane has been apparently employed in [24], while the road plane is the choice in [21].

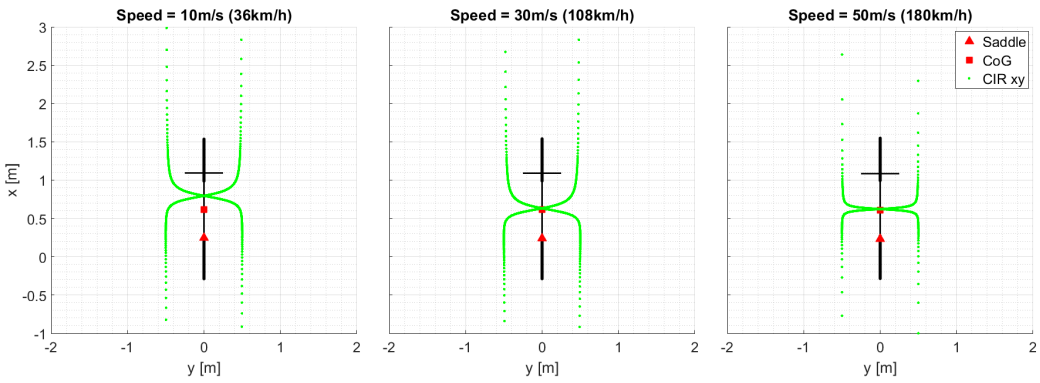

Figure 3. Velocity centres of weave in a transverse plane through the saddle point.

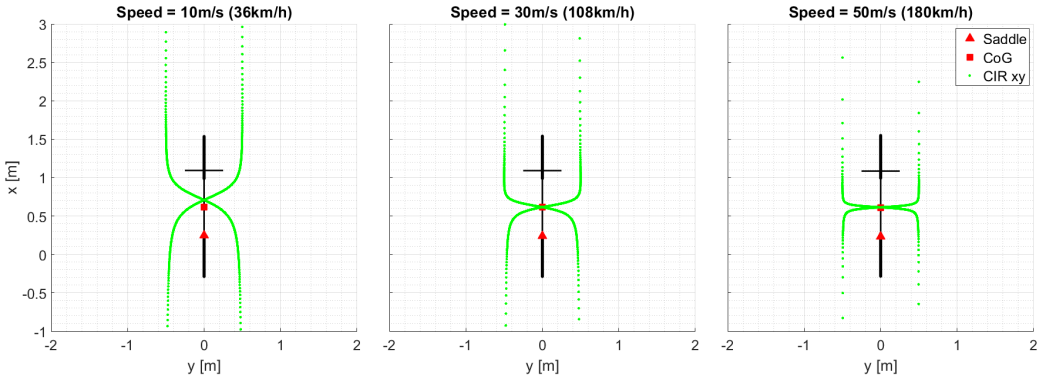

Figure 4. Velocity centres of weave in a transverse plane through the centre of mass.

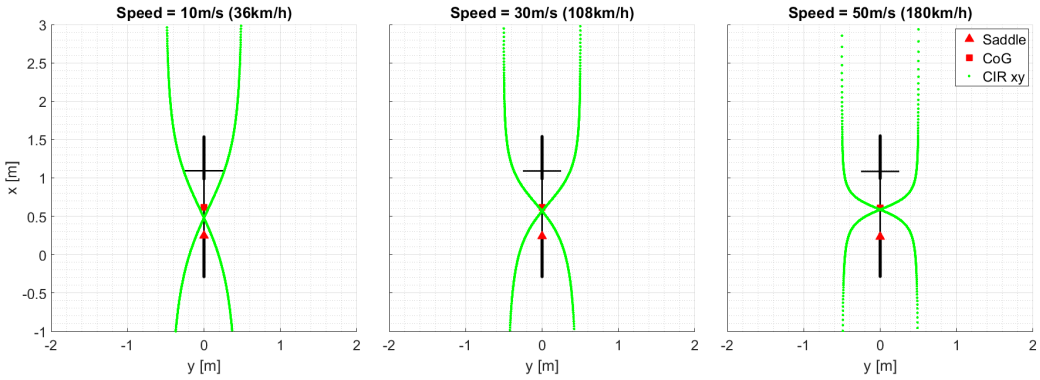

Figure 5. Velocity centres of weave in the road plane.

4.2. Front-View

Similarly to the analysis carried out in the top view, different choices are possible for the analysis from the frontal view as well.

When the plane through the saddle point (0.25 m ahead of the rear contact point in static condition) is considered, see Figure 6, the centrode intersection occurs below the road plane ($z = 0$), with the distance from the road plane increasing with the speed from 0.586 m up to 3.949–7.926 m at 10, 30 and 50 m/s, respectively—indeed the roll component reduces with respect to the lateral component.

When the reference is a plane through the centre of mass (0.62 m ahead of the rear contact point in static condition), see Figure 7, then the centrode intersection moves above the road plane, shifting from -0.349 to -0.586 m as the speed increases from 10 to 30 m/s, and then moving back towards the road plane until -0.555 m at 50 m/s.

Finally, in the case the reference plane being through the rear contact point, see Figure 8, the diagrams get closer to those with a reference on the saddle; this is not surprising since the two point are close in the longitudinal direction. The cross point moves from 1.209 m at 10 m/s up to 6.972–13.200 m at 30 and 50 m/s, respectively.

The same considerations related to the selection of the reference plane and reported at the end of the previous section still hold, although there are no references in the literature to compare the different options available.

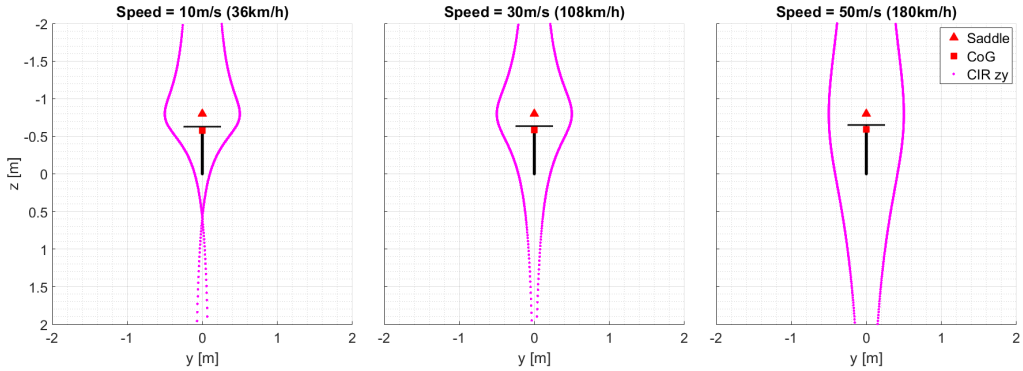

Figure 6. Velocity centres of weave in a frontal plane through the saddle.

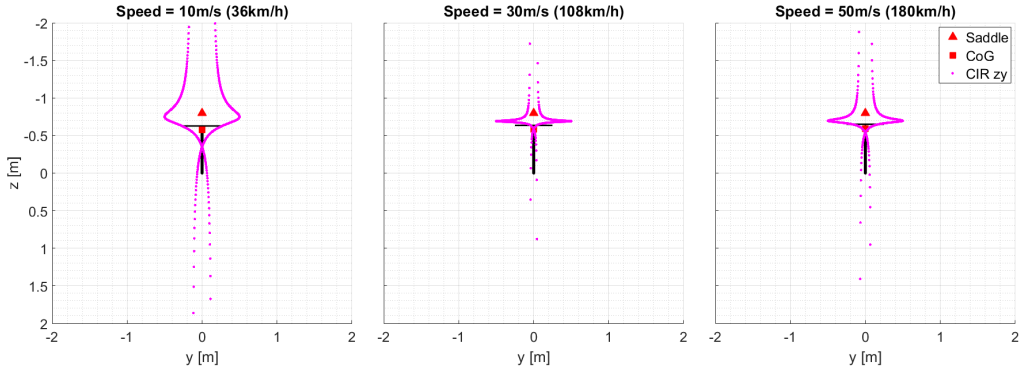

Figure 7. Velocity centres of weave in a frontal plane through the centre of mass.

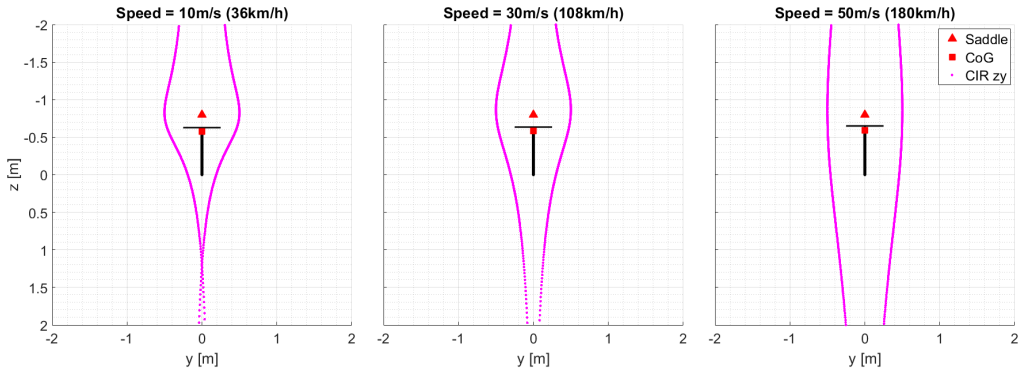

Figure 8. Velocity centres of weave in a frontal plane through the rear contact point.

5. Wobble

In this section the wobble mode shape is analysed in three transverse (top view) and three frontal (front view) planes, at different speeds. These are exactly the same planes considered for the weave in Section 4. The same scaling has also been applied to the eigenvectors, with the maximum saddle lateral displacement component equal to 0.5 m.

5.1. Top-View

Figure 9 shows the trajectory of the velocity centre (centrode) during the wobble oscillation, when the plane considered is through the saddle. The pattern undergoes minor variations when varying the speed: The trajectory cross point moves forward from 0.626 m up to 0.644–0.650 m at 10, 30 and 50 m/s, respectively—a slightly over-steer scenario, if we keep using the same convention employed in Section 4 (cross point ahead of the centre of mass).

Figure 10 shows the trajectory of the velocity centre projected on a transverse plane through the centre of mass. The results are similar to those described above, with the trajectory cross point again almost speed independent and moving from 0.587 m at 10 m/s to 0.571–0.585 m at 30 and 50 m/s, respectively—a slightly under-steering scenario (cross point behind the centre of mass).

Finally, the road plane is considered. In this case the results are those in Figure 11: The intersection appears behind the centre of mass, moving with a non-linear trend from 0.485 m at 10 m/s to 0.373–0.405 m at 30 and 50 m/s, respectively—following the nomenclature in Section 4 this wobble is called under-steering (cross point behind the centre of mass).

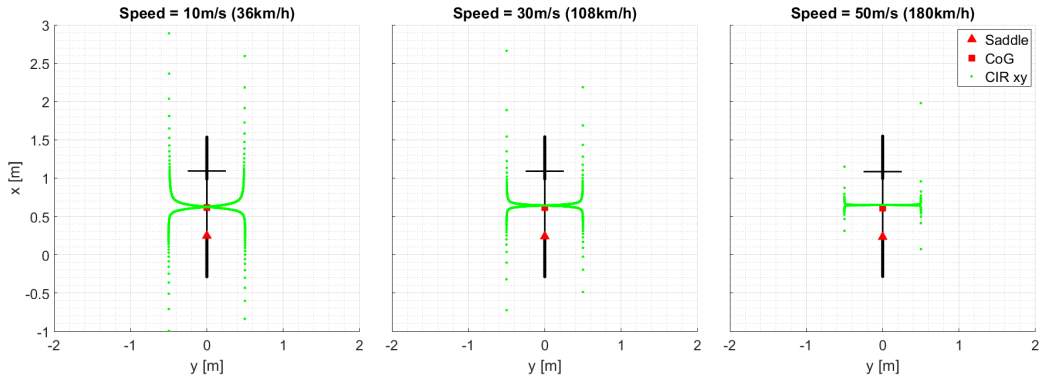

Figure 9. Velocity centres of wobble in a transverse plane through the saddle point.

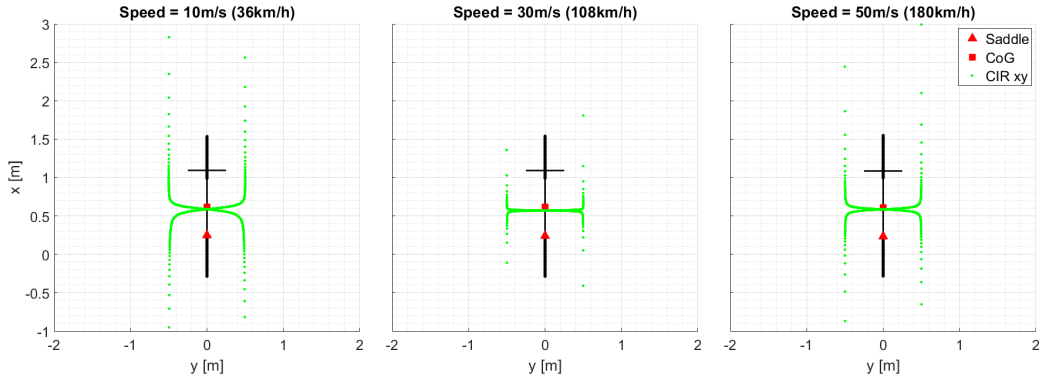

Figure 10. Velocity centres of wobble in a transverse plane through the centre of mass.

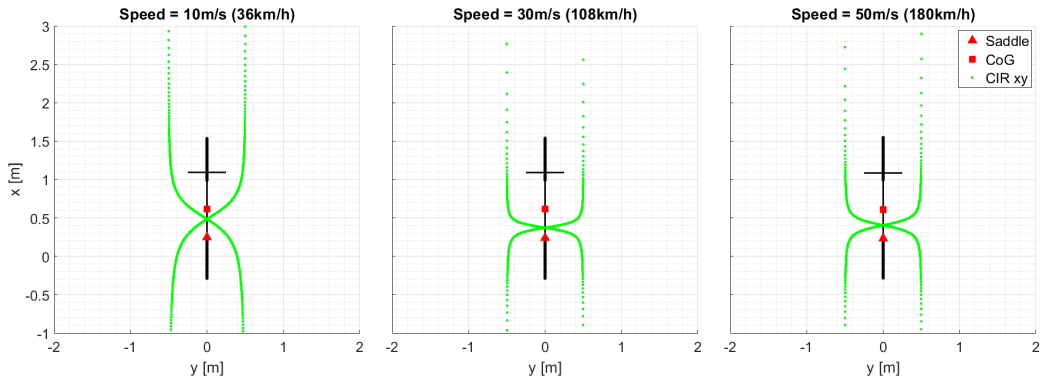

Figure 11. Velocity centres of wobble in the road plane.

5.2. Front-View

When the plane through the saddle point is considered, see Figure 12, the centrode intersection occurs below the road plane, with the distance from the road plane decreasing

from 1.355 to 0.383 m as the speed increases from 10 to 30 m/s.At high speeds (>30 m/s) the intersection distance slightly increases up to 0.555 m at 50 m/s.

When the reference is a plane through the centre of mass, see Figure 13, then the centrode intersection moves above the road plane, decreasing the height as the speed increases, moving from −0.753 m to −0.715/−0.673 m at 10, 30 and 50 m/s, respectively, and getting closer to the centre or mass.

Finally, in the case the reference plane is through the rear contact point, see Figure 14, the diagrams get closer to those with a reference on the saddle and the cross point moves from 2.756 m to 1.099–1.322 m at 10, 30 and 50 m/s, respectively—again this is not surprising since the two point are close in the longitudinal direction.

The same considerations related to the selection of the reference plane and reported at the end of the weave section still hold.

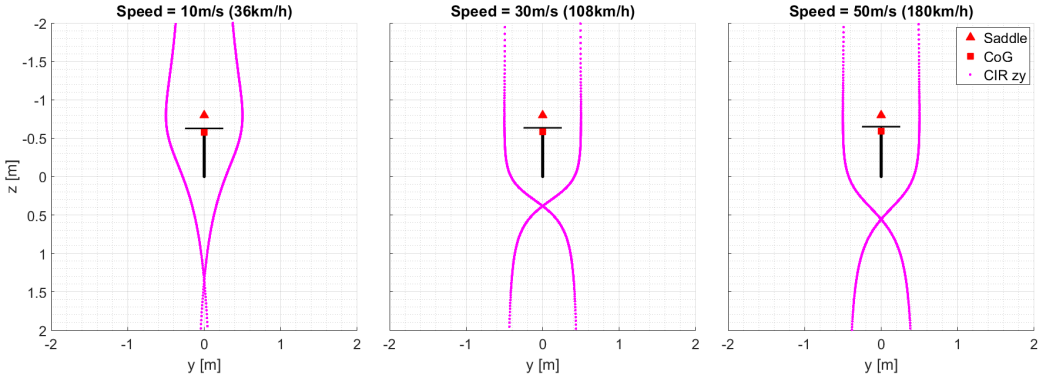

Figure 12. Velocity centres of wobble in a frontal plane through the saddle point.

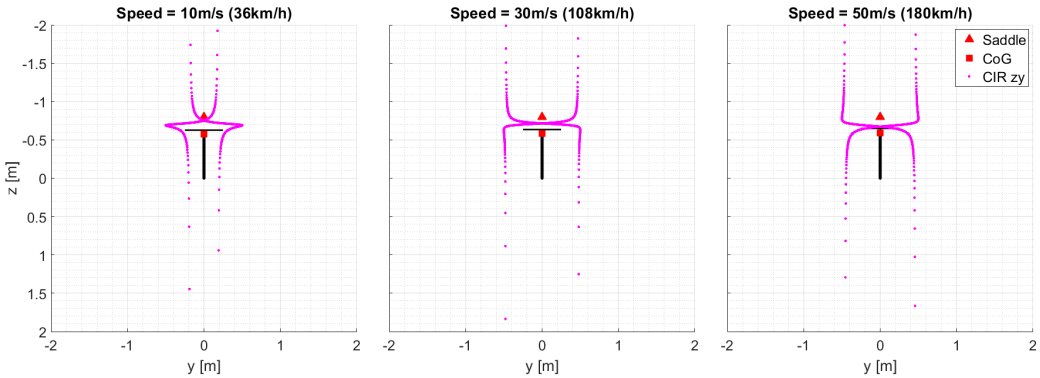

Figure 13. Velocity centres of wobble in a frontal plane through the centre of mass.

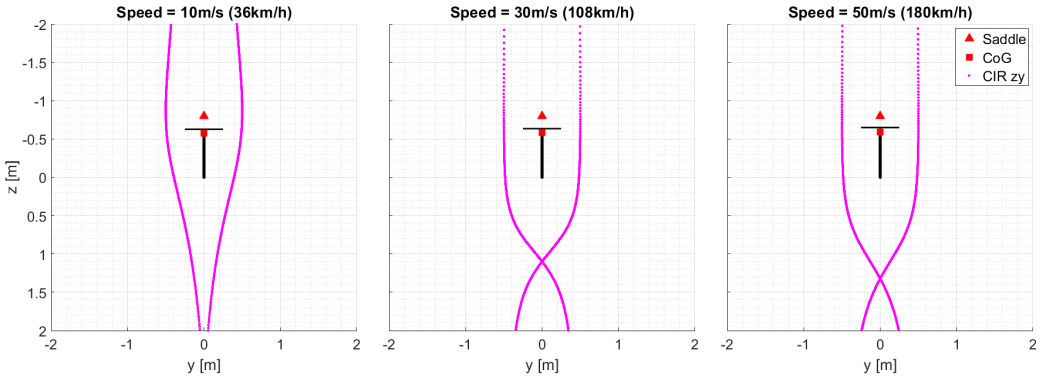

Figure 14. Velocity centres of wobble in a frontal plane through the rear contact point.

6. Conclusions

The mode shape of the most important lateral vibration modes of two-wheeled vehicles, namely weave and wobble, are analysed through a screw axis approach (instead of the classic compass diagram approach), which is an extension of the velocity centre approach recently proposed in the literature. The analyses reported in the literature have been extended to include also the frontal plane, in addition to the transverse plane, and wobble, in addition to weave. Finally, multiple transverse and frontal plane have been considered. It has been shown that different patterns can be obtained depending on the selected plane, and also different dynamic classifications, e.g., under- vs. over-steer behaviour.

This highlights the importance of choosing the appropriate reference plane to correlate the rider's sensations with the mode shapes: Saddle planes are closely related to the effective rider position, while centre of mass planes are related to the whole system dynamics. Both of these options are dependent on the motorcycle geometry, so another option is the use of the rear contact point planes, which do not change with the rider and bike.

Author Contributions: Conceptualization, M.B. and M.M.; methodology, M.B. and M.M.; software, M.B.; validation, M.B. and M.M.; formal analysis, M.B. and M.M.; investigation, M.B. and M.M.; resources, M.M.; writing—original draft preparation, M.B. and M.M.; writing—review and editing, M.B. and M.M.; supervision, M.M.; project administration, M.M. All authors have read and agreed to the published version of the manuscript.

Funding: This research received no external funding.

Conflicts of Interest: The authors declare no conflict of interest.

References

1. Sharp, R.S. The Stability and Control of Motorcycles. *J. Mech. Eng. Sci.* **1971**, *13*, 316–329. [CrossRef]
2. Sharp, R.S.; Evangelou, S.; Limebeer, D.J.N. Advances in the modelling of motorcycle dynamics. *Multibody Syst. Dyn.* **2004**, *12*, 251–283. [CrossRef]
3. Cossalter, V. *Motorcycle Dynamics*, 2nd ed.; Lulu.com: Morrisville, NC, USA, 2006.
4. Cossalter, V.; Lot, R.; Massaro, M. An advanced multibody code for handling and stability analysis of motorcycles. *Meccanica* **2011**, *46*, 943–958. [CrossRef]
5. Pacejka, H.; Besselink, I.J.M. *Tire and Vehicle Dynamics*, 3rd ed.; Butterworth-Heinemann: Oxford, UK, 2012.
6. Limebeer, D.J.N.; Massaro, M. *Dynamics and Optimal Control of Road Vehicles*; Oxford University Press: Oxford, UK, 2018.
7. Cossalter, V.; Lot, R.; Massaro, M. The influence of frame compliance and rider mobility on the scooter stability. *Veh. Syst. Dyn.* **2007**, *45*, 313–326. [CrossRef]
8. Passigato, F.; Eisele, A.; Wisselmann, D.; Gordner, A.; Diermeyer, F. Analysis of the Phenomena Causing Weave and Wobble in Two-Wheelers. *Appl. Sci.* **2020**, *10*, 6826. [CrossRef]
9. Bova, M.; Massaro, M.; Petrone, N. A Three-Dimensional Parametric Biomechanical Rider Model for Multibody Applications. *Appl. Sci.* **2020**, *10*, 4509. [CrossRef]
10. Nishimi, T.; Aoki, A.; Katayama, T. Analysis of Straight Running Stability of Motorcycles. *SAE Tech. Pap.* **1985**, *856124*, 1080–1094.
11. Katayama, T.; Aoki, A.; Nishimi, T.; Okayama, T. Measurements of structural properties of riders. *SAE Tech. Pap.* **1987** , *871229*, 1–9.
12. Doria, A.; Formentini, M.; Tognazzo, M. Experimental and numerical analysis of rider motion in weave conditions. *Veh. Syst. Dyn.* **2012**, *50*, 1247–1260. [CrossRef]
13. Uchiyama, H.; Tanaka, K.; Nakagawa, Y.; Kinbara, E.; Kageyama, I. Study on Weave Behavior Simulation of Motorcycles Considering Vibration Characteristics of Whole Body of Rider. 2018. Available online: https://saemobilus.sae.org/content/2018-32-0052/ (accessed on 8 August 2021).
14. Cossalter, V.; Doria, A.; Lot, R.; Massaro, M. The effect of rider's passive steering impedance on motorcycle stability: Identification and analysis. *Meccanica* **2011**, *46*, 279–292. [CrossRef]
15. Doria, A.; Marconi, E.; Massaro, M. Identification of rider's arms dynamic response and effects on bicycle stability. In Proceedings of the AMSE IDETC International Design Engineering Technical Conferences & Computers and Information in Engineering Conference, St. Louis, MO, USA, 17–19 August 2020.
16. Massaro, M.; Cole, D.J. Neuromuscular-Steering Dynamics: Motorcycle Riders vs. Car Drivers. In Proceedings of the ASME 2012 5th Annual Dynamic Systems and Control Conference, Fort Lauderdale, FL, USA, 31 October–2 November 2012; pp. 217–224.
17. Massaro, M.; Lot, R.; Cossalter, V.; Brendelson, J.; Sadauckas, J. Numerical and experimental investigation of passive rider effects on motorcycle weave. *Veh. Syst. Dyn.* **2012**, *50*, 215–227. [CrossRef]

18. Klinger, F.; Nusime, J.; Edelmann, J.; Plöchl, M. Wobble of a racing bicycle with a rider hands on and hands off the handlebar. *Veh. Syst. Dyn.* **2014**, *52*, 51–68. [CrossRef]
19. Marcolongo, R. Notizie Sul Discorso Matematico e Sulla vita di Giuio Mozzi. *Boll. Bibliogr. E Stor. Delle Sci. Mat.* **1905**, *8*, 1–8.
20. Shabana, A.A. *Dynamics of Multibody Systems*, 4th ed.; Cambridge University Press: Cambridge, UK, 2013.
21. Cossalter, V.; Doria, A. Analysis of motorcycle slalom manoeuvres using the Mozzi axis concept. *Veh. Syst. Dyn.* **2004**, *42*, 175–194. [CrossRef]
22. Cossalter, V.; Doria, A. Instantaneous screw axis of two-wheeled vehicles in typical manoeuvres. *Veh. Syst. Dyn.* **2006**, *44*, 669–678. [CrossRef]
23. Cossalter, V.; Bellati, A.; Doria, A.; Peretto, M. Analysis of racing motorcycle performance with additional considerations for the Mozzi axis. *Veh. Syst. Dyn.* **2008**, *46*, 815–826. [CrossRef]
24. Armanini, S.; Leo, E.; Pezzola, M.E.; Taroni, N.; Cheli, F. Riding velocity and payload conditions affecting weave modal shape: Subjective assessment on riding safety. In Proceedings of the Symposium on the Dynamics and Control of Single Track Vehicles, Padova, Italy, 9–11 September 2019.